Contents list available at IJRED website

Int. Journal of Renewable Energy Development (IJRED)

Journal homepage: http://ejournal.undip.ac.id/index.php/ijred

Research Article

A Novel PandO$_T$-Neville's Interpolation MPPT Scheme for Maximum PV System Energy Extraction

Muralidhar Nayak Bhukya[a] and Venkata Reddy Kota[b]

[a] *Department of Electrical and Electronics Engineering, Institute of Aeronautical Engineering, Hyderabad, 500043,*

[b] *Department of Electrical and Electronics Engineering, Jawaharlal Nehru Technological University, Kakinada, 533003.*

ABSTRACT. Photovoltaic (PV) system posses an optimal operating pointing, termed as Maximum Power Point (MPP). Using Maximum Power Point Tracking (MPPT) algorithm, MPP of PV system has to be tracked continuously in any climatic conditions. In general, traditional Perturb and Observe (PandO$_T$) MPP tracker is widely used among existing controllers. But, PandO$_T$ fails to harvest maximum power from solar panel, in addition oscillations around MPP results in low efficiency of the PV system. The contradiction involved in the traditional controller can be addressed as PandO$_T$ operates with a fixed step size. Hence, with large step size MPP can be reached quickly but the magnitude of oscillations around MPP are high. Similarly, when PandO$_T$ operated with tiny step size magnitude of oscillations can be reduced at the same time PV system consumes much time to reach MPP. In order to eliminate the contradiction involved with traditional MPPT scheme and effectively optimize PV system energy, this paper put forwards a hybrid MPPT scheme based on PandO$_T$ and Neville interpolation. The proposed scheme is executed in two stages. In the first stage, PandO$_T$ is operated with a large step size till the voltage reaches near to maximum point. In the second stage, Neville interpolation is used to find the maximum power point. The performance of the proposed scheme is compared with Golden Section Search (GSS) and PandO$_T$ MPPT controllers. With the proposed scheme the convergence time required to reach MPP is improved greatly. Experimental prototype is designed and developed to verify the performance of the proposed scheme. Experimental and simulation results provide enough evidence to show superiority of the proposed scheme.

Keywords: Photovoltaic (PV) system, Maximum Power Point Tracking (MPPT), Traditional Perturb and Observe(PandO$_T$), Neville Interpolation and Golden ratio

Article History: Received December 15th 2017; Received in revised form July 16th 2018; Accepted September 12th 2018; Available online
How to Cite This Article: Bhukya, M. N. and Kota, V. R. (2018) A Novel PandO$_T$-Neville's Interpolation MPPT Scheme for Maximum PV system energy extraction. International Journal of Renewable Energy Development, 7(3), 251-260
https://dx.doi.org/10.14710/ijred.7.3.251-260

1. Introduction

Among renewable energy sources Photovoltaic (PV) power generation is marked as a remarkable one due to eco-friendly nature, low maintenance, absences of rotating parts. The non-linear characteristic of PV module has an optimal operating point and dependent on solar irradiance and temperature. Tracking optimal operating point in any conditions is the responsibility of Maximum Power Point Tracking (MPPT) scheme. Hence, MPPT algorithm plays a vital role in optimizing PV power. From literature many MPPT controllers (Ali *et al.* 2013) – (Trishan *et al.* 2007) such as Perturb and Observe (Dezso *et al.* 2013) Hill-climbing method (Karatepe *et al.* 2010), Incremental Conductance (Chia *et al.* 2011) method, Open Circuit Voltage (Andrea *et al.* 2015), Short Circuit Current (Xu Di *et al.* 2014), Incremental Resistance Method (Qiang *et al.* 2011), Ripple Correlation Control (Solodovnik *et al.* 2004), Slide Mode Control (Kim II-Song *et al.* 2006), Neural Network (Veerachary *et al.* 2003) and Genetic Algorithm (Slimane *et al.* 2014) have been proposed.

[a] Corresponding author: rathode.muralidhar@gmail.com

Traditional Perturb and Observe (PandO$_T$) MPPT controller operation is based on perturbing with a fixed step size (Baltas *et al.* 1986). Based on perturbation PandO$_T$ is categorized into three types as, (i) Voltage based PandO$_T$ (Carannante *et al.* 2009) (ii) Current based PandO$_T$ (Abdelsalam *et al.* 2011) and (iii) direct duty ratio based PandO$_T$ (Sera D *et al.* 2008). Among existing controllers Perturb and Observe/ Hill Climbing methods are widely used in industrial and public sectors due to low cost and simple implementation (Alajmi *et al.* 2011). The minor difference between PandO$_T$ and Hill Climbing Method (HCM) is presented in (Eltawil *et al.* 2013), as HCM operation is based only on duty ratio. Apart from this, the major demerits associated with PandO$_T$ are slow response, confuses to decide optimal operating point of the PV system and oscillations in output power reduces efficiency (Subudhi *et al.* 2013).

The authors of (Xiao *et al.* 2006) – (Femia *et al.* 2008) have presented different strategies to improve the performances of PandO$_T$. In (Emilio *et al.* 2014), a simple two step algorithm is attached with PandO$_T$ for better efficiency. A modified PandO$_T$ is proposed in (Killi *et al.* 2015), to avoid drift in output power of the PV system. In (Kota et al. 2016), the performance of PandO$_T$ is

enhanced by estimating a voltage point near to the optimal operating point.

For standalone PV system, Incremental Conductance (INC) based MPPT scheme is generally preferred (Liu *et al.* 2008) due to drift free power generation during varying atmospheric conditions (Safari *et al.* 2011). Fractional Open Circuit Voltage (Adly *et al.* 2011) and Fractional Short Circuit Current methods (Masoum *et al.* 2002) are combined with other MPPT schemes to improve time response, steady state and dynamic performances of the PV system (Hart *et al.* 1984). Ripple Correlation (Casadci *et al.* 2006) and Slide Mode Controllers (de Brito *et al.* 2011) have successfully eliminated the drawbacks associated with traditional MPPT schemes. At the same time, fails to achieve Maximum Power Point (MPP) quickly during dynamic weather conditions (Koutroulis *et al.* 2001).

Hence, to avoid the demerits allied with existing MPPT methods, this paper put forwards a novel MPPT scheme combing PandO$_T$ with Neville Interpolation. The proposed scheme is executed in two stages. In the first stage, PandO$_T$ is operated with a large step size such that PV system converges quickly to the region of operating point. As it is well known that, PandO$_T$ oscillates around MPP with respect to step size provided initially to operate. The magnitude of oscillations clearly depends on the step size. In the second stage, three voltage points are chosen from the region around MPP and given as input for Neville Interpolation. Among these three voltage points, the Neville polynomial equations settle down to the exact MPP of PV system. Until there is a change in irradiance or temperature, MPP of PV system is maintained as constant. The contradiction involved in the traditional controller is eliminated with Neville Interpolation. The proposed scheme is compared with PandO$_T$ and GSS MPPT controllers. The test results provide enough evidence to prove superiority of the proposed scheme.

This paper is organized as follows: after brief introduction on traditional MPPT scheme drawbacks, mathematical modeling of PV cell is presented in Section 2. Proposed scheme along with PandO$_T$ and GSS controllers are presented in Section 3. Simulation results under real environmental conditions are presented in Section 4. Designed prototype with experimental results is presented in Section 5. And section 6 concludes the paper.

2. Mathematical Modeling of PV cell

The electrical equivalent circuit of a single diode Photovoltaic (PV) cell is shown in Fig. 1. PV cell is a combination of p-type and n-type semiconductor materials. When solar irradiance or equivalent energetic light is focused on PV module, free electrons are diffused to generate electric energy. Typically, PV cell posses low voltage hence PV cells are connected in series or parallel combination to meet the load rating. A simplified I-V characteristic equation is used in this paper to determine output current of PV cell and mathematically expressed as follows (Venkata *et al.* 2016)

$$I_{PV} = I_{SC}\left\{1-\alpha_1\left[\exp\left(\frac{V_{PV}}{\alpha_2 V_{OC}}\right)-1\right]\right\} \quad (1)$$

The two coefficients 'α_1' and 'α_2' are described as

$$\alpha_1 = \left(1-\frac{I_M}{I_{SC}}\right)\exp\left(\frac{-V_M}{\alpha_2 V_{OC}}\right) \quad (2)$$

$$\alpha_2 = \left(\frac{V_M}{V_{OC}}-1\right)/\log\left(1-\frac{I_M}{I_{SC}}\right) \quad (3)$$

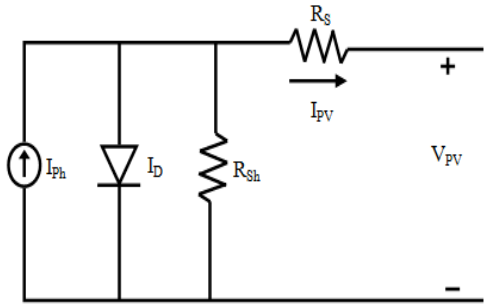

Fig. 1 Single Diode PV Cell

where V_M, I_M, V_{OC} and I_{SC} are given by equations (4) - (7)

$$V_M = V_{M,STC}\left[\log(e+0.5\Delta G)(1-0.0028\Delta T)\right] \quad (4)$$

$$I_M = I_{M,STC}\left[\frac{G}{G_{STC}}(1+0.025\Delta T)\right] \quad (5)$$

$$V_{OC} = V_{OC,STC}\left[\log(e+0.5\Delta G)(1-0.0028\Delta T)\right] \quad (6)$$

$$I_{OC} = I_{OC,STC}\left[\frac{G}{G_{STC}}(1+0.025\Delta T)\right] \quad (7)$$

Table 1
RNG-100D PV panel specifications

Parameter	Symbol	Value
Maximum Power	P_{Max}	100Watt
Maximum Voltage	V_{Max}	18.5V
Maximum Current	I_{Max}	5.29A
Open Circuit Voltage	V_{OC}	22.5V
Short Circuit Current	I_{SC}	5.75A

where:

- I_{PV} is output current of PV (A),
- I_{SC} is short circuit current of PV (A),
- V_{PV} is output voltage of PV (V),
- V_{OC} is open circuit voltage of PV (V),
- α_1 and α_2 are coefficients of I-V equation,
- V_M is maximum output voltage of PV (V),
- I_M is maximum output current of PV (A),
- $V_{M,STC}$ is maximum voltage at Standard Test Conditions (STC),
- $I_{M,STC}$ is maximum current at STC,
- $V_{OC,STC}$ is open circuit voltage at STC,
- $I_{SC,STC}$ is short circuit current at STC,
- $\Delta G = G/G_{STC} - 1$,
- G is irradiance on the panel surface (W/m^2),
- G_{STC} is irradiance at STC (1000 W/m^2),
- $\Delta T = T - T_{STC}$,
- T is temperature on the panel surface (°C),
- T_{STC} is temperature at STC (25°C).

The nonlinear I-V and P-V characteristics of RNG-100D 100Watt mono-crystalline PV panel at different irradiance and temperatures is shown in Fig. 2 and corresponding PV panel specifications are presented in Table 1.

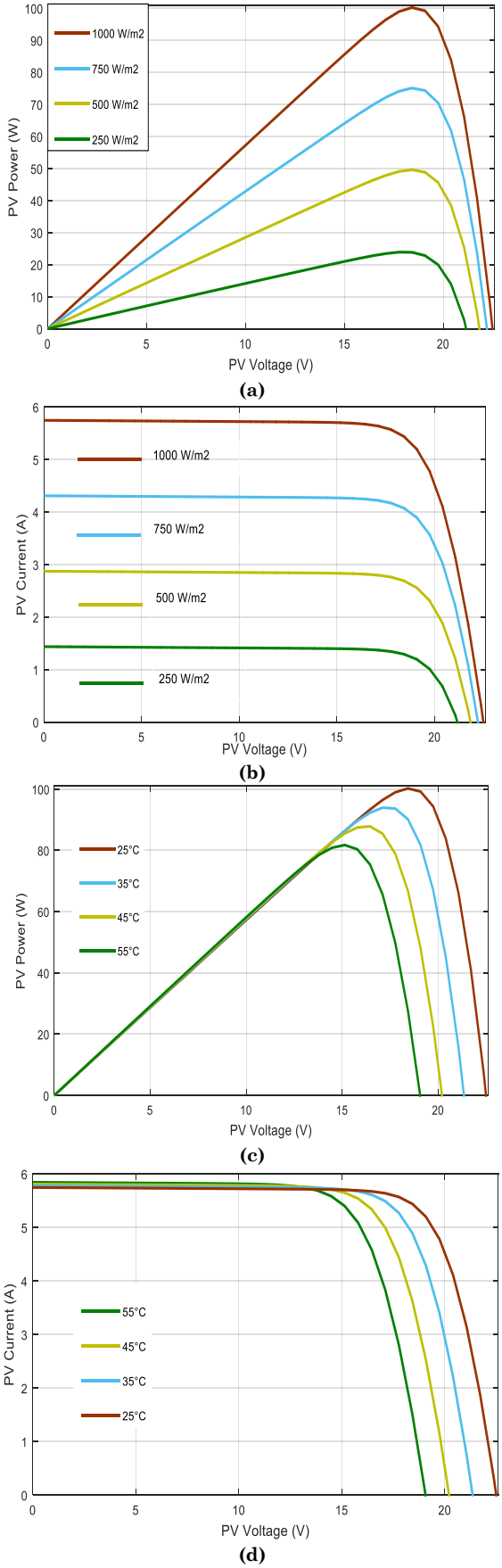

Fig. 2 Non-linear P-V and I-V characteristics at different (a)-(b)irradiance and (c)-(d)temperatures

3. Dc-dc SEPIC Converter

The electrical equivalent circuit of a dc-dc Single Ended Primary Inductor Converter (SEPIC) is shown in Fig. 3. The converter has the capability to step-up or step-down the supply voltage. The converter is employed with filter capacitor (C_f), inductor (L_1, L_2), capacitors (C_1, C_2), MOSFET (M) as switching operator and Diode (D) (Killi et al. 2015).

Operation of the converter is separated into two as Continuous Conduction Mode and Discontinuous Conduction Mode. If the current passing through inductor L_1 is equal to zero, converter is operating in Discontinuous Conduction Mode. During Continuous Conduction Mode of operation, inductor L_1 is always greater than zero. For a duty cycle more than 50%, converter boosts the supply voltage and vice versa if the duty cycle is less than 50%. Duty cycle of the converter is given as

$$\frac{V_{Load}}{V_{PV}} = \frac{D}{1-D} \tag{8}$$

where 'D' is duty cycle, V_{PV} is panel voltage and V_{Load} is output voltage of the converter. SEPIC converter parameters used in this paper is illustrated in Table 2.

Table 2
Dc-dc SEPIC converter parameters

Parameter	Symbol	Value
Filter Capacitor	C_f	440µF
Inductor	L_1, L_2	180µH, 180µH
Capacitor	C_1, C_2	47µF, 220µF
MOSFET	M	600V, 40A, 1.5V
Diode	D	600V, 15A, 0.4V

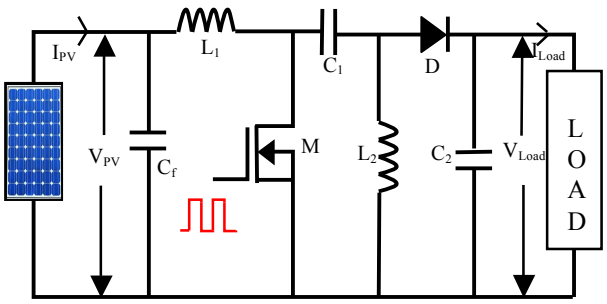

Fig. 3 Electrical equivalent circuit of SEPIC converter

4. Maximum Power Point Tracking Schemes

4.1 Traditional perturb and observe (PandO$_T$)

The PandO$_T$ MPPT algorithm is widely used among traditional controllers (Femia *et al.* 2008) due to simplicity and low cost implementation. PandO$_T$ perturbs with fixed step size and observes power at each perturbation to decide direction of perturbation as shown in the below formulae.

$$P(m) > P(m\text{-}1) \rightarrow \text{Forward direction} \tag{9a}$$

$$P(m) < P(m\text{-}1) \rightarrow \text{Reverse direction} \tag{9b}$$

where P(m) and P(m-1) are power harvested after and before perturbations. The flowchart of PandO$_T$ controller is depicted in Fig. 4 (Trishan *et al.* 2007) The demerits allied with the PandO$_T$ scheme are more time to reach

MPP, low efficiency, oscillations in steady state and dynamic states.

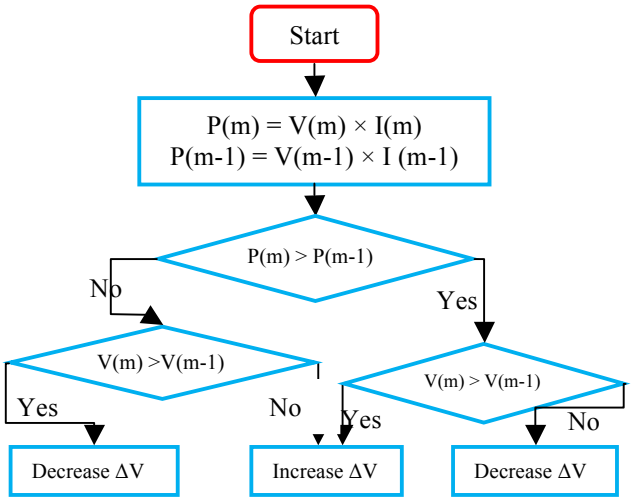

Fig. 4 Traditional Perturb and Observe Controller Flowchart

4.2 Golden Section Search (GSS)

In (Kheldoun *et al.* 2016), presented a novel MPPT scheme based on Golden Ratio. At first, based on PV system open circuit voltage a closed interval [0, V_{OC}] is selected. And thereafter, two voltage points V_1 and V_2 are generated in the closed interval as

$$\left.\begin{aligned} V_1 &= a + 0.618(b-a) \\ V_2 &= b - 0.618(b-a) \end{aligned}\right\} \quad (10)$$

In continuation, powers at V_1 and V_2 are compared to decide next closed interval either [V_1, V_{OC}] or [0, V_2]. Therefore, it is worth to conclude that closed interval initial selected [0, V_{OC}] is reduced at each iteration until $|V_2-V_1| \leq \varepsilon$ is achieved. In normal conditions, GSS gives acceptable performance but fails to cope MPP under real environmental conditions. Flowchart of the GSS MPPT scheme is shown in Fig. 5.

4.2.1 Step-by-step procedure involved in GSS

(a) Based on open circuit voltage, select closed interval [0, V_{OC}]
(b) From Eq. (10), two voltage points are generated in the closed interval
(c) Powers at voltage V_1 and V_2 are compared to decide next interval.
If $P(V_1) > P(V_2)$, the closed interval is updated as [0, V_2] or else [V_1, V_{OC}]
(d) Again, from (a) to (c) procedure is repeated
(e) Once the condition, $|V_2-V_1| \leq \varepsilon$ is attained. The procedure converged to MPP.
(f) At every change in irradiance and temperature closed interval has to be updated.

4.3 Proposed scheme

From literature, the contradiction involved in PandO$_T$ is addressed as PV system perturbed with large step size reaches MPP quickly but the magnitudes of oscillations around MPP are high. At the same time, tiny step size impacts the magnitude of oscillations effectively but consumes much time to reach necessary operating point as shown in Fig. 6.

In order to eliminate the contradictions associated with traditional perturb and observe controller, this paper presents a novel MPPT scheme based on PandO$_T$ and Neville Interpolation. The proposed scheme is executed in two stages.

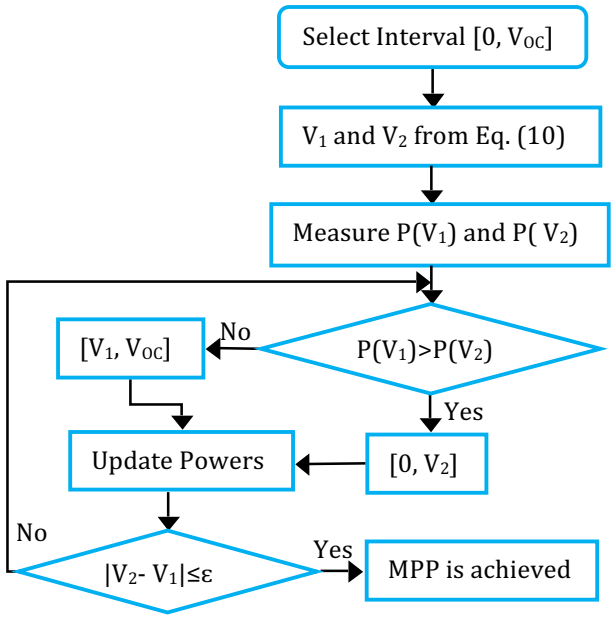

Fig. 5 GSS Flowchart

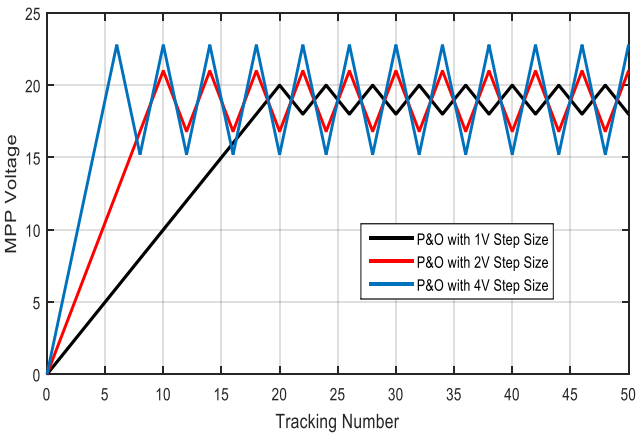

Fig. 6 MPP tracking using PandO$_T$ for different step sizes

Stage I:

Initially, PV system is operated with traditional PandO$_T$ controller with a large step size of 4 Volts to achieve MPP region within a precise time. After approaching MPP region, traditional controller oscillates in both forward and reverse directions around MPP. At that instant three voltage points are noted as shown in Fig. 7. These three voltage points are chosen as input for the second stage.

Stage II:

For better convenience these three voltage points are simplified as

$$\left.\begin{aligned} V_2 &= V \\ V_1 &= V_2 - \Delta V \\ V_0 &= V_1 - 2\Delta V \end{aligned}\right\} \quad (11)$$

In the second stage, these three voltage points are chosen as the inputs for Neville Interpolation. And the intermediate steps involved in the proposal are depicted in Fig. 9.

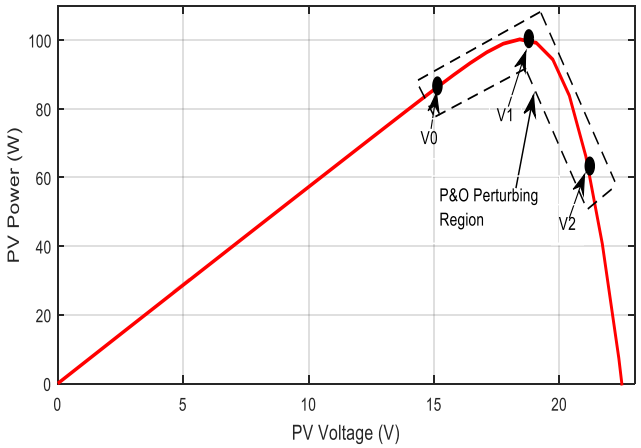

Fig. 7 At MPP, perturbation in forward and reverse directions.

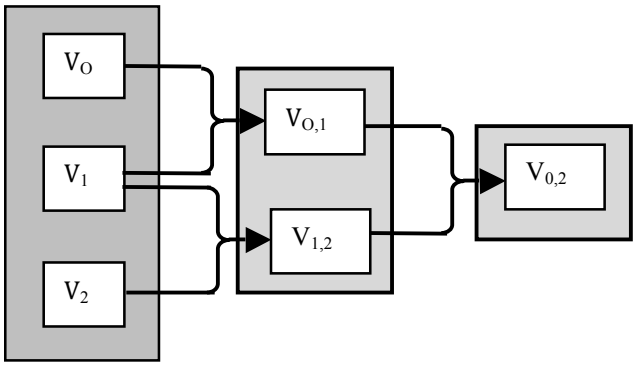

Fig. 9 Intermediate steps involved in Neville Interpolation

From V_0, V_1 and V_2 the intermediate interpolation polynomial equations '$V_{0,1}$' and '$V_{1,2}$' are expressed as a function of power as

$$P(V_{0,1}) = \frac{(V_1 - V)P_0(V_0) + (V - V_0)P_1(V_1)}{V_1 - V_0} \quad (12)$$

$$P(V_{1,2}) = \frac{(V_2 - V)P_1(V_1) + (V - V_1)P_2(V_2)}{V_2 - V_1} \quad (13)$$

Finally, the Neville Interpolation polynomials in terms of intermediate is as follows

$$P(V_{0,2}) = \frac{(V_2 - V)P(V_{0,1}) + (V - V_0)P(V_{1,2})}{V_2 - V_0} \quad (14)$$

We get V_{MPP}, when $\frac{d\lfloor P(V_{0,2})\rfloor}{dV} = 0$

$$\frac{d\lfloor P(V_{0,2})\rfloor}{dV} = \frac{(V_2 - V)(V_1 - V)}{(V_2 - V)(V_1 - V_0)}P_0(V_0) - \frac{(V_2 - V)(V_0 - V)}{(V_2 - V)(V_1 - V_0)}P_1(V_1) - \frac{(V_1 - V)(V_2 - V)}{(V_2 - V_1)(V_2 - V_0)}P_0(V_0) + \frac{(V_1 - V)(V_0 - V)}{(V_2 - V_1)(V_1 - V_0)}P_2(V_2) \quad (15)$$

Therefore Eq. (15) can be simplified as

$$V_{MPP} = \frac{A(V_1 + V_2) + B(V_0 + V_2) + C(V_0 + V_1)}{2(A + B + C)} \quad (16)$$

where

$$A = \frac{P_0(V_0)}{(V_0 - V_1)(V_0 - V_2)},$$

$$B = \frac{P_1(V_1)}{(V_1 - V_0)(V_1 - V_2)} \text{ and}$$

$$C = \frac{P_2(V_2)}{(V_2 - V_0)(V_2 - V_1)}$$

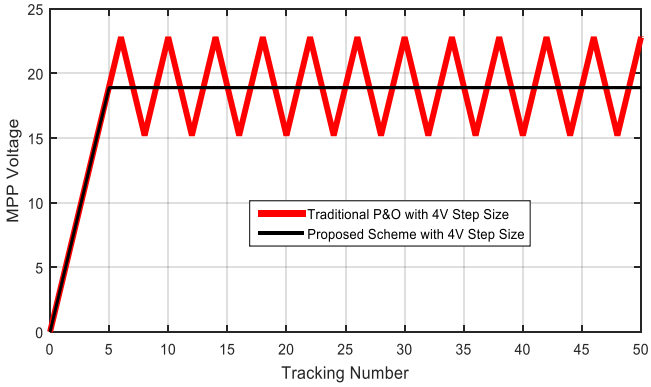

Fig. 10 Comparison between traditional PandO and proposed scheme

The polynomial equations settle down the sampling points to exact MPP of PV system. After achieving V_{MPP} from Neville Interpolation, PV system duty cycle is maintained constant until there is a change in irradiance or temperature on the panel surface. A simple comparison between PandO$_T$ operated with 4V step size and proposed scheme is presented in Fig. 10. Error correcting loop helps to cope with actual power locus during change in irradiance and temperature. After

acheving maximum power, the proposed scheme is perturbed around MPP with a small step size of 0.1V *i.e.* δV.

The flow chart depicted in Fig. 11 clearly summaries the working of the proposed MPPT scheme. The proposed scheme is simple and easy to implement. In addition achieves MPP with in a precise time and avoids the drawbacks associated with PandO$_T$ and GSS. A 3-Dimensional view of MPP obtained from the proposed Neville Interpolation scheme at different irradiance and temperatures levels is plotted in Fig. 12.

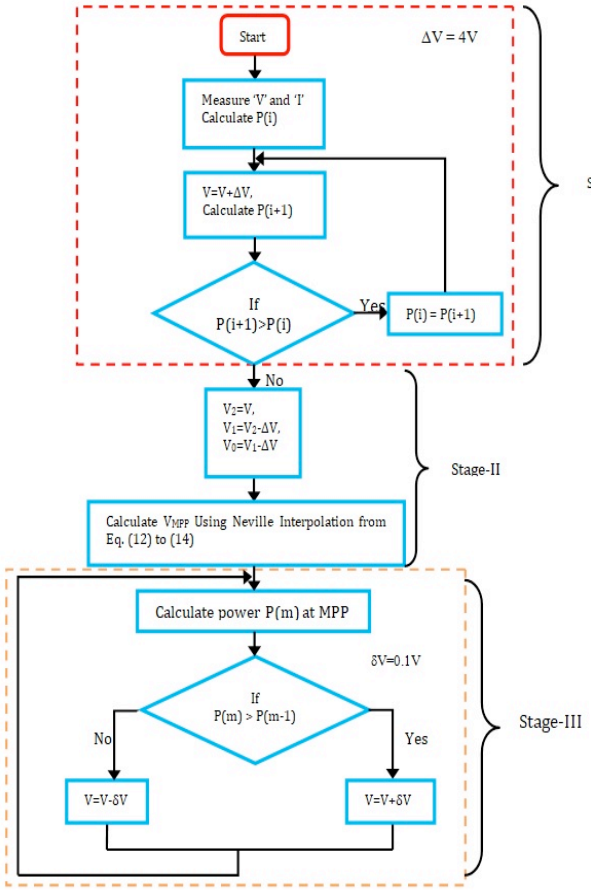

Fig. 11 Proposed MPPT scheme flowchart

6. Simulation Results

Initially, MPPT schemes are developed in MATLAB/SIMULINK. Simulating at a particular irradiance or temperature value doesn't project effective working of any MPPT scheme. Hence, in this paper MPPT schemes are simulated under real environmental conditions. Using CS300-L silicon cell pyranometer, every change in irradiance and temperature are noted for a duration of eight hours as plotted in Fig. 13 (a) and (b). Initially, the irradiance profile shown in Fig. 13(a) is started with a minimum irradiance of 138.131W/m^2 at a temperature of 27.606°C. After a time period of 0.145 Sec the profile experiences a maximum irradiance of 729.906 W/m^2 with a temperature of 32.731°C. During the testing period temperature on PV system is observed in between 27.5°C to 34°C as shown in Fig. 13(b).

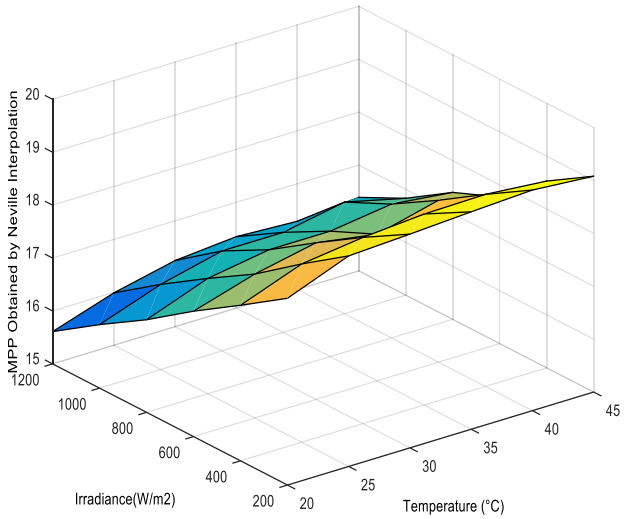

Fig. 12 3-Dimensional view of voltages obtained using the proposed MPPT scheme

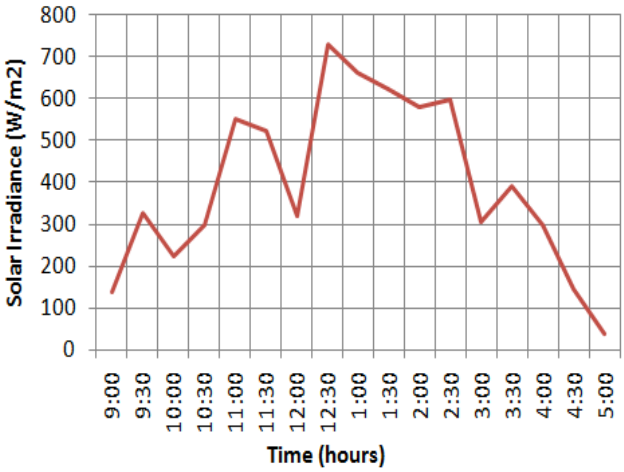

(a)

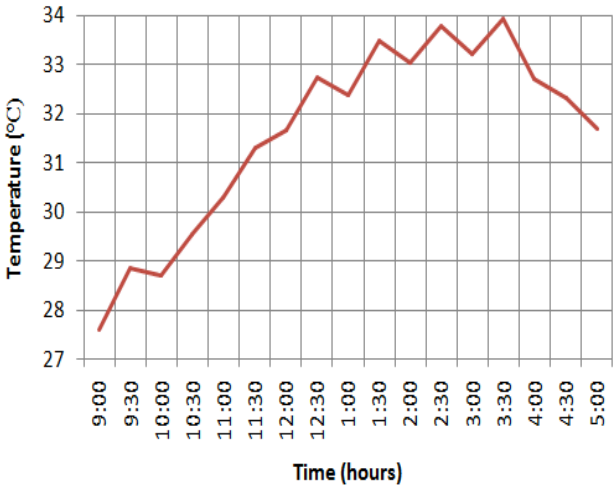

(b)

Fig. 13 Real environmental profiles (a) Irradiance and (b) Temperature

Fig. 14 shows PV system output current using different MPPT schemes. From P-V and I-V characteristics in Fig. 3, it can be concluded that irradiance on the panel surface is directly proportional to PV current. Hence, change in irradiance effects the shape

of PV current. From figure, it is clearly visible that magnitude of oscillations in PandO$_T$ are very high, on the other hand GSS fail to track the current locus path perfectly. While, the proposed MPPT scheme tracks the locus path perfectly without any oscillations. Similarly, PV system output voltage and power are illustrated in Fig. 15 and 16. It is worth to conclude the analysis of the simulation test as the proposed MPPT scheme harvests maximum power from PV system compared to GSS and PandO$_T$. During low irradiance level GSS fail to optimize power locus, whereas PandO$_T$ tracks the locus with oscillations. A detailed comparison of MPPT schemes under real environmental conditions is depicted in Table 3. At the same time efficiency are plotted in Fig. 17.

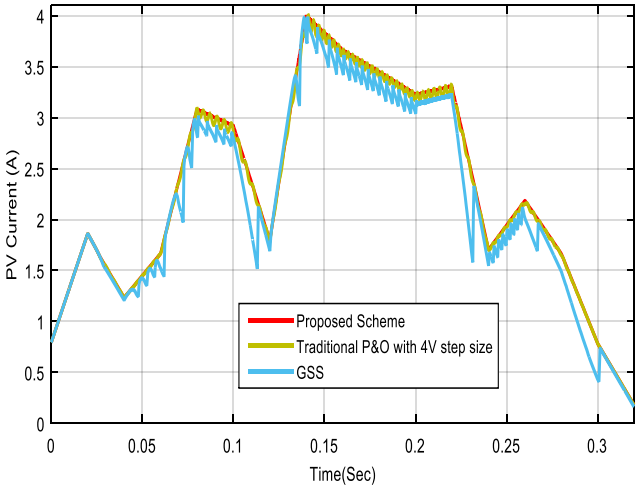

Fig. 14 Output current of PV system

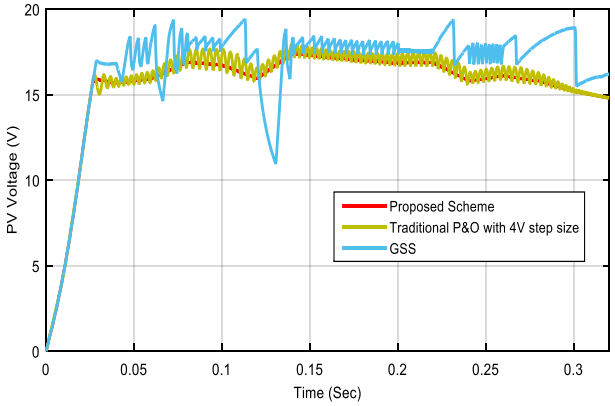

Fig. 15 Output voltage of PV system

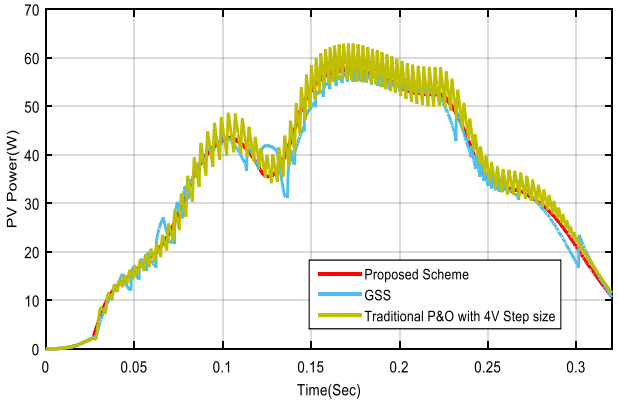

Fig. 16 Output Power of PV system

Tabel 3
MPPT performance comparison during real environmental conditions

S.No	Time (hrs)	G(W/m²)	T(°C)	Actual Power	V_{MPP}	I_{MPP}	V_{OC}	I_{SC}	Power(W) Obtained using			Efficiency (%)		
									PandO	GSS	Proposed Scheme	η_{PandO}	η_{GSS}	$\eta_{Proposed\ Scheme}$
1	09:00	138.131	27.606	12.36	17.11	0.7	20.3	0.8	11.31	12	12.2	91.5	97	98.7
2	09:30	327.713	28.865	31.18	17.77	1.7	21	1.9	30.04	30.13	30.9	96.3	96.6	99.1
3	10:00	221.837	28.706	20.56	17.77	1.1	20.6	1.28	19.51	19.9	20.1	94.8	96.7	97.7
4	10:30	298.45	29.547	28.03	17.77	1.5	20.8	1.172	26.98	27.15	27.8	96.2	96.8	99.1
5	11:00	551.515	30.283	53.15	17.77	2.9	21.3	3.2	51.35	52.2	53.05	96.6	98.2	99.8
6	11:30	523.066	31.301	49.93	17.77	2.8	21.2	3	47.875	48.93	49.7	95.8	97.9	99.5
7	12:00	320.681	31.658	29.83	17.11	1.7	20.6	1.85	28.45	28.88	29.1	95.3	96.8	97.5
8	12:30	729.906	32.731	59.6	17.77	3.9	21.3	4.23	55.25	58.65	59.34	92.7	98.4	99.5
9	01:00	662.803	32.382	53.28	17.77	3.5	21.3	3.85	42.33	49.95	53.11	79.4	93.7	99.6
10	01:30	623.597	33.482	48.96	17.77	3.3	21.1	3.61	38.01	45.25	48.6	77.6	92.4	99.2
11	02:00	580.941	33.029	44.96	17.77	3.0	21.1	3.37	39.4	41.75	44.72	87.6	92.8	99.4
12	02:30	596.882	33.791	36.18	17.77	3.1	21	3.45	29.13	32.45	36	80.5	89.6	99.5
13	03:00	305.495	33.22	28.04	17.11	1.6	20.4	1.77	26.25	26.99	27.8	93.6	96.2	99.1
14	03:30	391.095	33.941	36.24	17.11	2.1	20.6	2.27	34.7	35.19	35.98	95.7	97.1	99.2
15	04:00	298.46	32.717	27.2	17.77	1.5	20.5	1.73	26	26.15	27.1	95.5	96.1	99.6
16	04:30	143.142	32.331	12.42	17.11	0.7	19.8	0.83	11.43	11.37	12.3	92.02	91.5	99.03
17	05:00	37.613	31.699	2.67	15.79	0.1	18.4	0.22	0.97	1.72	2.5	36.3	64.4	93.6

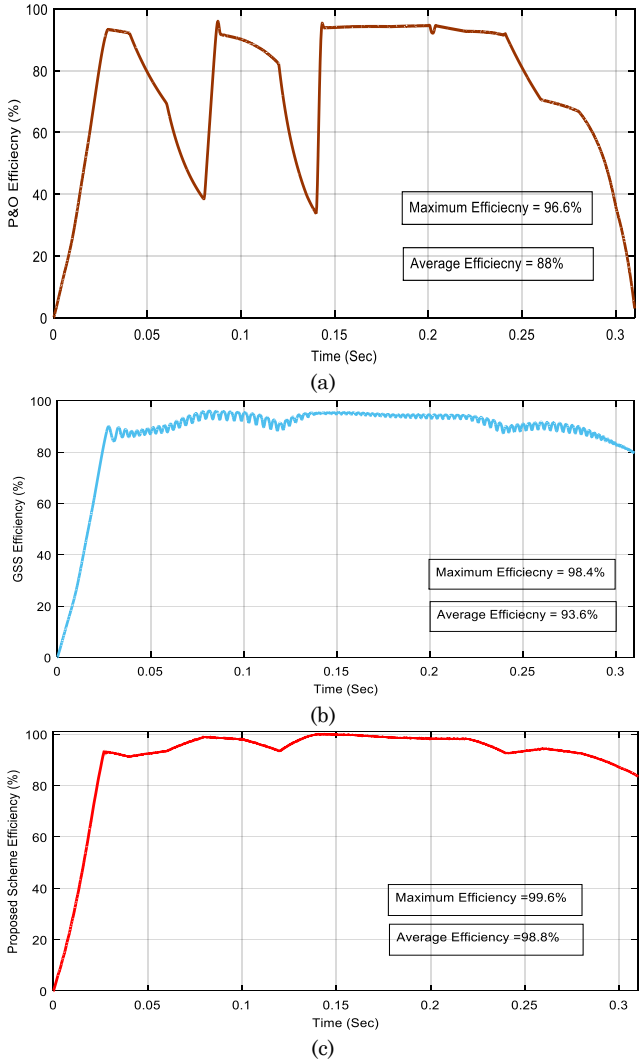

Fig. 17 Efficiency (a) PandO (b) GSS and (c) Proposed scheme(c)

7. Experimental Validation

To validate the performance of the proposed MPPT scheme a prototype is designed and developed. PV system parameters used for simulation and experimentation are same as depicted in Table 1 and 2. The solar panel is connected to SEPIC converter through Hall effect LA25-P current sensor and 7840 IC based voltage sensing circuit. The proposed scheme is programmed in DSP 30F4011 microcontroller and obtained pulses are given to 4081IC based PWM generator. In order to reduce losses between sensors and microcontroller TL084 buffer IC is employed. From PWM IC gate pulses are driven to switching device. Overall voltage and current protection is supervised by 4027 and 4098 flip-flop IC circuit.

Steady state performance of the proposed scheme is shown in Fig. 18. During this test PV system experiences an irradiance and temperature of 298 W/m2 and 28.5°C. For this particular irradiance and temperature values PV system has the capability to deliver a maximum power of 28Watt, with a maximum current and voltage of 1.5A and 17 V. The proposed scheme is succeeded in extracting maximum current, voltage and power at steady state performance.

The performance of the proposed scheme during raise in irradiance is plotted in Fig. 19. Initially, irradiance and temperature on the panel surface are increased from G=620 W/m2 and T=33.1°C to G=660W/m2 and T=32.8°C. The proposed scheme has a quick response in its output power. At, G=620 W/m2 and T=33.1°C PV system output parameters are PMax=60W, VMax=17.7V and IMax=3.2A. Correspondingly, at G=660W/m2 and T=32.8°C, PV system parameters are PMax=70W, VMax=18V and IMax=3.5A. from Fig. 19, it is clearly noticeable that the proposed scheme tracks maximum power path perfectly during change in irradiance. Similarly, Fig. 20 shows the performance of the proposed scheme during decrease in irradiance. At this test temperature on the panel is approximately same i.e., T=33°C and irradiance is changed from 390W/m2 to 335W/m2. From the experimental results it is evident that the proposed scheme harvest at most power from PV system in any weather conditions. In Table 4, performance of the proposed scheme is compared with PandOT and GSS controllers.

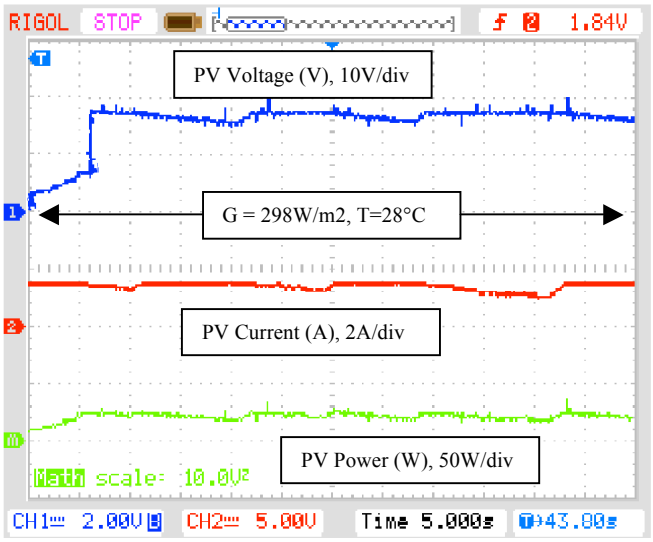

Fig. 18 Steady state performance of the proposed scheme

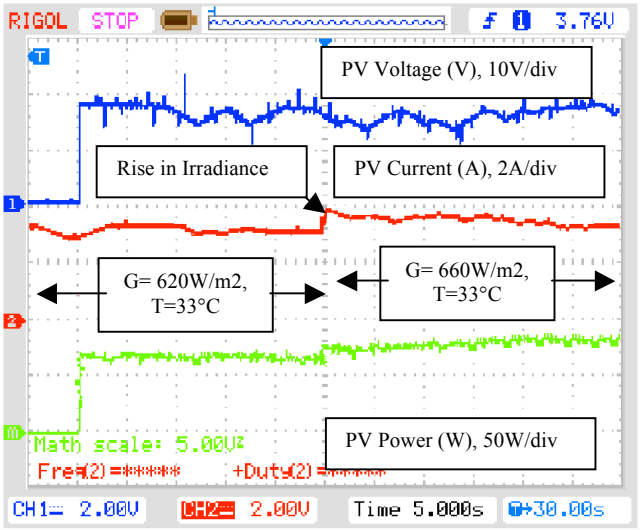

Fig. 19 MPPT performance at raise in irradiance

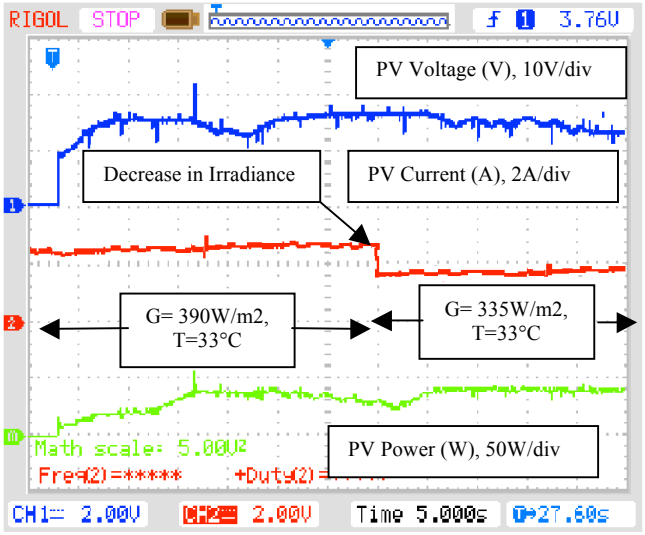

Fig. 20 MPPT performance at decrease in irradiance

Tabel 4
Performance comparison of the proposed MPPT scheme

Parameter	MPPT Scheme		
	PandOT	GSS	Proposed scheme
Implementation complexity	Simple	Medium	Simple
Tracking Speed	Low	Medium	Very High
System Dependency	Dependent	Independent	Independent
Reliability	Very Low	Medium	High
Efficiency	Low	High(during Normal conditions) Low(during Low Irradiation Levels)	High

8. Conclusion

This paper put forwards a novel MPPT scheme combing PandOT and Neville Interpolation to optimize steady state performance of the traditional controller, which is far superior to PandOT and GSS. The proposed scheme is executed in two stages. In the first stage, MPP region is reached using PandOT with a large step size of 4V. And in the second stage, exact MPP is attained by Neville Interpolation. Hence, the proposed scheme has improved steady state performance of the PandOT controller effectively. From the simulation and experimental results, it is evident that the proposed scheme is far superior to the traditional PandO and GSS MPPT controllers.

References

Ali-Reza, R., Moradi, Md-H., Shahriar, J. (2013) Classification and Comparison of Maximum Power Point Tracking techniques for Photovoltaic System: A Review, *Renewable and Sustainable Energy Reviews*, 9, 433-443.

Trishan, E., Patrick, L. C. (2007) Comparison of Photovoltaic Array Maximum Power Point Tracking techniques, *IEEE Transaction on Energy Conversion,* 22(2), 439-449.

Dezso, S., Laszlo, M., Tamas, K., Sergiu, V., Remus, T. (2013) On the Perturb-and-Observe and Incremental Conductance MPPT methods for PV system, *IEEE Journal of Photovoltaics*, 3(3), 1070-1078.

Karatepe, E. S., Hiyama, T. (2010) Simple and High- efficiency photovoltaic system under non-uniform operating conditions, *IET Renewable Power Generation*, 4(4), 354-368.

Chia-Hung, L., Cong-Hui, H., Yi-Chun, D., and Jian-Livng, C. (2011) Maximum photovoltaic power tracking for the PV array using fractional–order incremental conductance method, *Applied Energy*, 88(12), 4840-4847.

Andrea, M., and Andrew, R. K. (2015) Maximum Power Point Tracking converter based on the Open Circuit voltage method for Thermoelectric Generators, *IEEE Transaction on Power Electronics*, 30(2), 828-839.

Xu, D., Ma, Y., and Chen, Q. (2014) A global maximum power point tracking method based on interval short circuit current, *European Conference on Power Electronics and Applications*, DOI:10.1109/EPE.2014.69107 24.

Qiang, M., Mingwei, S., Liying, L., and Josep, M. G. (2011) A novel improved variable step-size Incremental-Resistance MPPT method for PV systems, *IEEE Transaction on Industrial Electronics*, 50(4), 749-758.

Solodornik, E., and Liu, S. D. R. (2004) Power controller design for maximum power tracking in solar installation. *IEEE Transaction on Power Electronics*, 19(5), 1295-1304.

Kim-II, S., Kim, M., Youn, M. (2006) New Maximum Power Point Tracker using Sliding-Mode observer for estimation of solar array current in the grid-connected photovoltaic system, *IEEE Transaction on Industrial Electronics,* 53(4), 1027-1035.

Veerachary, M., Senjyu, T., and Uezato, K. (2003) Neural Network based maximum-power-point-tracking of coupled inductor interleaved-boost-converter-supplied PV system using Fuzzy Controller. *IEEE Transaction on Industrial Electronics*, 50(4), 749-758.

Slimane, H., Jean-Paul, G., and Fateh, K. (2014) Experimental analysis of genetic algorithm based MPPT for PV systems, *International Renewable and Sustainable Energy Conference*, 7-12, DOI: 10.1109/IRSEC.2014.7059887.

Baltas, P., Tortoreli, M., Russell, PE. (1986) Evaluation of power output for fixed and step tracking photovoltaic arrays. *Solar Energy*, 37(2), 147-163.

Carannante, G., Fraddano, C., Pagano, M., Piegari, L. (2009) Experimental performance of MPPT algorithm for photovoltaic sources subjest to inhomogeneous insolation, *IEEE Transaction on Industrial Electronics*, 56(11), 4374-80.

Abdelsalam, AK., Massoud, AM., Ahmed, S., Enjeti, PN. (2011) High performance adaptive perturb and observe MPPT technique for photovoltaic based micro-grids. *IEEE Transaction on Power Electronics*, 26(4), 1010-21.

Sera, D., Teodorescu, R., Hantschel, J., and Knoll, M. (2008) Optimized maximum power point tracker for fast changing environmental conditions. *IEEE Transaction on Industrial Electronics*, 55(7), 2629-37.

Alajmi, BN., Ahmed, KH., Finney, SJ., Williams, BW. (2011) Fuzzy-logic-control approach of a modified hill-climbing method for maximum power point in microgrid standalone photovoltaic system. *IEEE Transaction on Power Electronics*, 26(4), 1022-30.

Eltawil, A. Mohamed., and Zhengming, Zhao. (2013) MPPT techniques for photovoltaic applications, *Renewable and Sustainable Energy Reviews*, 25, 793-813.

Subudhi, B., and Pradhan, R., (2013) A comparative study on maximum power point tracking techniques for photovoltaic arrays. *IEEE Trans. on Sustainable Energy,* 4(1), 89-98.

Xiao, W., Lind, M. G. J., Dunford, WG., Capel, A. (2006) Real-time identification of optimal operating point in photovoltaic power systems. *IEEE Trans. on Industrial Ele.*, 53(4), 1017-1026.

Femia, N., Lisi, G., Petrone, G., Spagnudo, G., and Vitelli, M. (2008) Distributed maximum power point tracking of photovoltaic arrays: novel approach and system analysis, *IEEE Transaction on Industrial Electronics*, 55(7), 2610-21.

Emilio, M., Giovanni, P., and Giovanni, S. (2014) A two steps algorithm improving the PandO steady state MPPT efficiency, *Applied Energy,* 113, 414-421.

Muralidhar, K., and Susovon, S. (2015) Modified Perturb and Observe MPPT Algorithm for Drift Avoidance in Photovoltaic Systems. *IEEE Transactions on Industrial Electronics*, 62(9), 5549-5559.

Venkata, R. K., and Muralidhar, N. B. (2016) A novel linear tangents based PandO scheme for MPPT of a PV system. DOI.org/10.1016/j.rser.2016.12.054.

Liu, F., Duan, S., Liu, F., Liu, B., and Kang, Y. (2008) A variable step size INC MPPT method for PV systems. *IEEE Transaction on Industrial Electronics,* 55(7), 2622-2628.

Safari, A., Mekhilef, S. (2011). Simulation and hardware implementation of incremental conductance MPPT with direct control method using CUK converter. *IEEE Transaction on Industrial Electronics*, 58(4), 1154-1161.

Adly, M., El-Sherif, H., Ibrahim, M., (2011) Maximum Power Point Tracker for a PV cell using Fuzzy agent adapted by the fractional open circuit voltage technique. In: *proceedings of the IEEE international conference on fuzzy systems*, 1918-22.

Masoum, MAS., Dehbonei, H., Fuchs, EF. (2002) Theoretical and experimental analyses of photovoltaic systems with voltage and current based maximum power point tracking. *IEEE Transaction on Energy Conversion,* 17(4), 514-522.

Hart, GW., Branz, HM., Cox, CH. (1984) Experimental tests of open loop maximum power point tracking techniques, *Solar Cells*, 13, 185-95.

Casadei, D. Grandi, G., Rossi, C. (2006) Single-Phase Single-Stage photovoltaic generation system based on ripple correlation control maximum power point tracking, *IEEE Transaction on Energy Conversion,* 21, 562-8.

de Brito, MAG., Sampaio, LP., Luigi, G., E Melo, GA., Canesin, CA. (2011) Comparative analysis of MPPT technique for PV applications. *In: proceedings of 2011 International Conference on Clean Electrical Power (ICCEP),* 99-104.

Koutroulis, E., Kalaitzakis, K., Voulgaris, NC., (2001) Development of a microcontroller based photovoltaic maximum power point tracking control system, *IEEE Transaction on Power Electronics,* 16(21), 46-54.

Venkata, R. K, Muralidhar, N. B. (2016) "A Simple and Efficient MPPT Scheme for PV Module using 2-Dimensional Lookup Table". pp.1-7, IEEE Power and Energy Conference at Illinois (PECI), DOI:10. 1109/PECI.20 16.7459226.